
Mechanism discovery with thermodynamically consistent and atom conserving chemical reaction neural networks

Anonymous Author(s)

Affiliation

Address

email

Abstract

1 Chemical reaction neural networks are a promising tool for the automated discovery
2 of chemical mechanisms from reactor data. For the first time, thermodynamic
3 consistency of the discovered mechanisms is enforced through DE DONDER hard-
4 constraints, leading to physical plausibility, improved convergence, and guaranteed
5 evolution towards the physically correct equilibrium composition.

6 1 Introduction

7 Machine learning has emerged as an important tool in chemistry discovery, reduction and acceleration [1]. An outstanding example is the Chemical Reaction Neural Network (CRNN), a *white-box*
8 neural network-twin of the classical chemical reaction network that allows autonomous discovery of
9 unknown reaction pathways [2]. Despite widely used in (bio-)chemical engineering [2–5], pyroly-
10 sis [6–8], combustion [9–11], as well as battery [12–16] and high energy material decomposition [17–
11 21], neither the CRNN nor its atom conserving variant, the AC-CRNN [3], are thermodynamically
12 consistent. Therefore, despite the potential of the approach, poor performances are obtained when the
13 local conditions approach the chemical equilibrium.
14

15 We present Thermodynamically Consistent CRNNs (TC-CRNNs) that leverage DE DONDER con-
16 straints to guarantee the physical plausibility and thermodynamic consistency of discovered mech-
17 anisms. For comparability, we will showcase the superior TC-CRNN performance using the Searson
18 mechanism, a standard example for mechanism discovery often used as a CRNN benchmark [2–4].

19 2 Related work

20 Besides numerous application to bulk-reactive systems, the CRNN was recently adapted to discover
21 the kinetics of surface reactive systems [22–24], which are extremely important to the chemical
22 industry. Uncertainty quantification has been applied [4, 5, 14, 15], allowing the estimation of predic-
23 tion and parameter accuracy, further enabling the development of automated, data-driven design of
24 experiment procedures [25]. However, none of these applications include hard-constraints to enforce
25 the physical plausibility of the discovered parameters. Recently, atom conservation was enforced
26 by a dedicated atom conservation layer, yielding the so-called AC-CRNN [3]. Here, we propose
27 the additional usage of DE DONDER constraints to guarantee thermodynamic consistency. This
28 strategy has already proven very successful in the context of Global Reaction Neural Networks [26–
29 28], which provide surrogates of steady state surface kinetics to accelerate industrial-scale reactor
30 simulations [29].

3 Method

CRNNs encode the commonly used law of mass action together with Arrhenius-type kinetics in linearized form

$$\vec{r}_j = \exp \left[\sum_i n_{i,j} \ln a_i + \ln A_{0,j} - \frac{E_{A,j}}{RT} + b_j \ln T \right] \quad (\text{Law of Mass Action \& Arrhenius Law})$$

with the rate r of reaction j , the pre-exponential factor A_0 , the universal gas constant R , the temperature T , temperature exponent b , reaction orders $n_{i,j} = \text{ReLU}(-\nu_{i,j})$, stoichiometric coefficients ν , and activities a_i of chemical species i [2].

Net rates of species production $\dot{s}_i = \sum_j \nu_{i,j} r_j$ are obtained by multiplication of the rates with stoichiometric coefficients. In contrast to classical methods, the stoichiometries of elementary reactions are not defined by the user but discovered. The AC-CRNN [3] further enforces atom conservation by a dedicated atom conservation layer which multiplies the stoichiometric coefficients of so-called key species with the matrix B^* which is derived from the elemental composition of each species.

However, the (AC)-CRNN is still not thermodynamically consistent because it handles activation energies and pre-exponential factors as independent fitting parameters. In reality, the parameters of forward and reverse reactions are related by thermodynamics, as described by the DE DONDER equation [30], which expresses effective rates r_{eff} as a function of forward reaction rates \vec{r} as

$$r_{\text{eff}} = \vec{r} \times \left(1 - \frac{Q}{K} \right) \quad (\text{DE DONDER constraint})$$

where, $Q = \prod_i a_i^{\nu_{i,j}}$ represents the species activities a for a reaction defined by the learnable stoichiometric coefficients ν , and K is the equilibrium constant which is calculated with tabulated thermodynamical properties. We enforce the thermodynamic consistency by embedding the DE DONDER equation as a hard constraint within the model structure (Fig. 1).

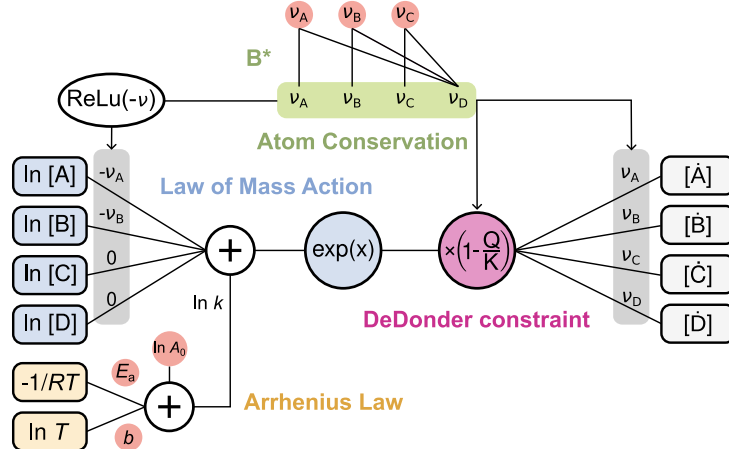
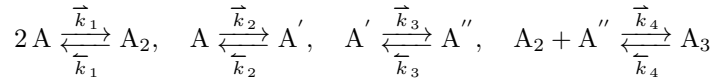


Figure 1: Schematic representation of the Thermodynamically Consistent Chemical Reaction Neural Network (TC-CRNN). In addition to the **Law of Mass Action**, the **Arrhenius Law**, and **atom conservation** already embedded in the AC-CRNN, the TC-CRNN also enforces thermodynamic consistency through the **DE DONDER constraint**. Learnable parameters (E_A , A_0 , b , ν) are marked red.

Models are trained in a neural ordinary differential equation setting [31] using reactor data obtained from the benchmark mechanism by SEARSON *et al.* [32]. It consists of four reactions of the chemical species A , A_2 , A' , A'' , and A_3 . Here, we consider also the reverse reactions



with reaction constants $k = T^b \cdot \exp(-E_A/RT)$ and values for forward \bar{k} , and reverse \bar{k} reaction of [0.2, 0.4, 0.26, 0.6] and [0.05, 0.1, 0.065, 0.15], respectively. K is calculated as $\exp(-\Delta_R G/RT)$

56 with $\Delta_R G = \sum_i \nu_{i,j} G_i$ and G_i of $[1.0, 0.6137, -0.3863, -1.773, -2.545] \cdot RT$ for the five species. In
 57 analogy to the original CRNN work, stoichiometric coefficients are uniformly random initialized
 58 between 0 and 0.1, and pre-exponential factors are initialized between $\exp(-10)$ and $\exp(-9.9)$.
 59 The Tsit5 ode solver implemented in *Julia* version 1.6.7 is used to solve concentration profiles with
 60 initial values of zero for A' , A'' , and A_3 and uniformly random initial values between 1.0 and 1.2
 61 for A and A_2 . 20 profiles are used for training by sampling them every two seconds for a maximum
 62 reaction time of 50 seconds. 5 % gaussian noise is applied to the obtained concentrations to mimic
 63 experimental measurement uncertainty. *Adamw* optimizer is employed for 15000 epochs with a
 64 learning rate of 0.01 for the first 1000 epochs and 0.001 afterwards, an exponential decay for the first
 65 (0.9) and the second (0.999) momentum estimate, and a weight decay of 10^{-8} . The loss function is
 66 the mean absolute deviation of concentrations divided by the maximum concentration per species
 67 found in the training data.

68 4 Results and Discussion

69 The new TC-CRNN is benchmarked against the standard CRNN and its atom conserving version
 70 called AC-CRNN by extracting the underlying mechanism from simulated experimental data of a
 71 SEARSON reaction system [32]. All three models accurately learn the systems behavior (Fig. 2). The
 72 only visible difference between the predicted concentration profiles is that the standard CRNN shows
 73 a mass balance error of several percent in the training range. In contrast, the AC-CRNN satisfies the
 74 mass and atom balance by design and therefore shows a mass balance error of 0 % for any initial
 75 condition and reaction time. The TC-CRNN implements the same atom conservation hard constraints
 76 as the AC-CRNN and therefore also closes the mass and atom balance under any condition.

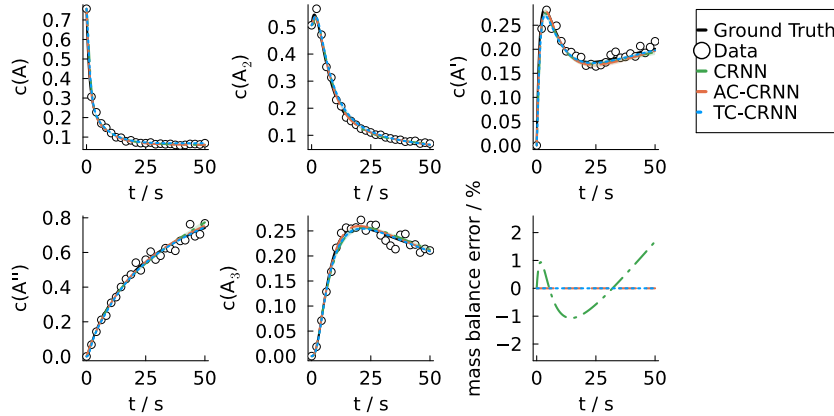


Figure 2: Concentration profiles and overall mass balance predicted by three CRNN model variants (lines) discovered from noisy reactor data (symbols) shown for one of the 20 training experiments.

77 The advantage of the TC-CRNN becomes apparent when the models are extrapolated to reaction
 78 times of $10 \times$ the training range. At long reaction times, the concentrations of all species reach the
 79 equilibrium composition (Fig. 3). The concentrations predicted by the standard CRNN significantly
 80 deviate from the ground truth for reaction times larger than 100 seconds as indicated by the relative
 81 error e_{rel} (Tab. 1). Also, the standard deviation σ between ten CRNN models with different initial
 82 parameter values increases significantly (Tab. 1). Instead of reaching a plateau value, the predicted
 83 concentrations keep changing even at the end of the extrapolation interval. Importantly, the mass

Table 1: Quantitative comparison of the CRNN model variants.

Model	$N_{\text{params}} \downarrow$	$\sigma/\mu (t=500 \text{ s}) \downarrow$	$e_{\text{rel}} (t=500 \text{ s}) \downarrow$
CRNN	48	235 %	526 %
AC-CRNN	40	155 %	238 %
TC-CRNN	20	0.123 %	0.172 %

balance error of the predicted solutions increases beyond 50 %, clearly indicating the physical inconsistency of the standard CRNN. The AC-CRNN, instead, conserves mass even under extrapolation conditions. The standard deviation between the predictions of ten differently initialized AC-CRNNs is of significantly smaller magnitude as for the CRNN (Tab. 1), but still not acceptable, as it is comparable to the ground truth concentration values and mean predictions μ for species A' and A_3 . The TC-CRNN predictions, in contrast, are accurate even for extrapolation. They conserve mass and evolve towards the correct chemical equilibrium by design. Standard deviations are negligible (Tab. 1) as all models lead to the same result.

Overall, TC-CRNNs enforce thermodynamic consistency through DE DONDER hard-constraints, which automatically determine the parameters of reverse reactions rather than learning them independently. This effectively halves the number of adjustable parameters N_{params} while simultaneously improving prediction uncertainty and accuracy under extrapolation (Tab. 1).

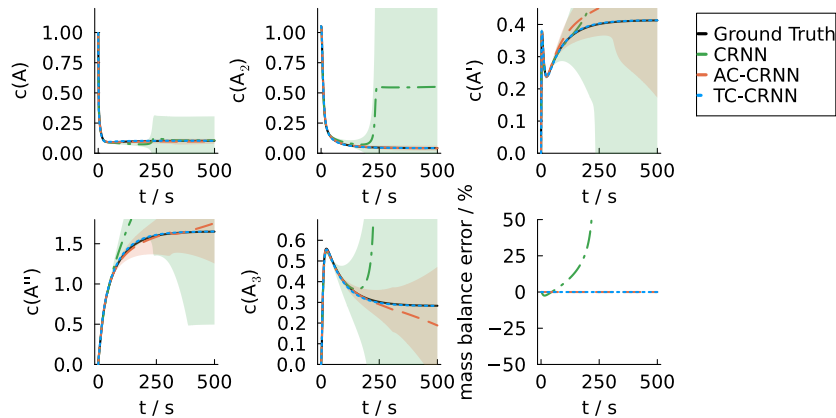


Figure 3: Concentration profiles and overall mass balance predicted by three CRNN model variants (lines) in an extrapolation setting with an unseen initial condition. Shaded areas indicate the standard deviation of ten differently initialized models each.

96 5 Conclusions and Future Work

We present the TC-CRNN framework which enables automated, atom conserving, and thermodynamically consistent mechanism discovery from reactor data. It is derived from the AC-CRNN by embedding DE DONDER hard-constraints into the model structure. We demonstrate that TC-CRNNs outperform CRNNs and AC-CRNNs in prediction accuracy, model variance, and extrapolation performance when trained with noisy reactor data from a SEARSON reaction system. Notably, the TC-CRNN replaces 50 % of the CRNN parameters with physical hard-constraints, indicating that it could handle larger and more complex reaction mechanisms.

Although this work focused on capturing concentration dynamics, the TC-CRNN is further guaranteed to predict consistent temperature changes as the required thermodynamics are already embedded into its architecture. For example, the adiabatic temperature rise relevant to the safety of chemical reactors does not have to be explicitly learned, making it an attractive tool for the chemical industry.

Considering also its characteristic to correctly predict dynamic equilibria by design, we believe that the TC-CRNN will become relevant to many fields the standard CRNN has not yet found wide adoption to, such as systems biology, atmospheric chemistry, and heterogeneous catalysis. Those fields are currently experiencing a rapid growth of available kinetic data, driven by digitalization, high-throughput experimentation, and emerging data infrastructures. The TC-CRNN provides a principled way to leverage these ever-growing datasets, ensuring that data-driven mechanism discovery remains consistent with fundamental physical laws.

115 6 Reproducibility

The code to fully reproduce all shown results will be made public together with the trained models.

117 **References**

- 118 [1] T. Echekki, A. Farooq, M. Ihme, S. M. Sarathy in *Machine Learning and Its Application*
119 *to Reacting Flows: ML and Combustion*, (Eds.: N. Swaminathan, A. Parente), Springer
120 International Publishing, Cham, **2023**, pp. 117–147.
- 121 [2] W. Ji, S. Deng, *Journal of Physical Chemistry A* **2021**, *125*, 1082–1092.
- 122 [3] F. A. Döppel, M. Votsmeier, *Proceedings of the Combustion Institute* **2024**, *40*, 105507.
- 123 [4] Q. Li, H. Chen, B. C. Koenig, S. Deng, *Physical Chemistry Chemical Physics* **2023**, *25*,
124 3707–3717.
- 125 [5] E. Nieves, R. Dandekar, C. Rackauckas, *Frontiers in Systems Biology* **2024**, *4*.
- 126 [6] W. Ji, F. Richter, M. J. Gollner, S. Deng, *Combustion and Flame* **2022**, *240*, 111992.
- 127 [7] C. Zhai, X. Wang, S. Zhang, Z. Cao, *Combustion and Flame* **2024**, *270*, 113798.
- 128 [8] Y. Zhong, W. Gao, C. Li, Y. Ding, *Bioresource Technology* **2025**, *429*, 132530.
- 129 [9] J. Huang, Y. Zhou, W. A. Yong, *Journal of Computational Physics* **2022**, *448*, 110743.
- 130 [10] W. Ji, X. Su, B. Pang, Y. Li, Z. Ren, S. Deng, *Fuel* **2022**, *324*, 124560.
- 131 [11] X. Su, W. Ji, J. An, Z. Ren, S. Deng, C. K. Law, *Combustion and Flame* **2023**, *251*, 112732.
- 132 [12] B. C. Koenig, P. Zhao, S. Deng, *Journal of Power Sources* **2023**, *581*, 233443.
- 133 [13] S. Bhatnagar, A. Comerford, Z. Xu, D. B. Polato, A. Banaeizadeh, A. Ferraris, *Journal of*
134 *Power Sources* **2025**, *628*, 235834.
- 135 [14] B. C. Koenig, H. Chen, Q. Li, P. Zhao, S. Deng, *Proceedings of the Combustion Institute* **2024**,
136 *40*, 105243.
- 137 [15] B. C. Koenig, P. Zhao, S. Deng, *Chemical Engineering Journal* **2025**, *507*.
- 138 [16] J. Zhang, C. Ma, S. Liu, Q. Guo, S. Liu, P. Han, Z. Huang, D. Han, *Cell Reports Physical*
139 *Science* **2025**, *6*, 102563.
- 140 [17] H. Wang, Y. Xu, M. Wen, W. Wang, Q. Chu, S. Yan, S. Xu, D. Chen, *Journal of Analytical*
141 *and Applied Pyrolysis* **2023**, *169*, 105860.
- 142 [18] G. Tang, H. Wang, C. Chen, Y. Xu, D. Chen, D. Wang, Y. Luo, X. Li, *RSC Advances* **2022**, *12*,
143 24163–24171.
- 144 [19] Y. Xu, Q. Chu, X. Chang, H. Wang, S. Wang, S. Xu, D. Chen, *Chemical Engineering Science* **2023**, *282*, 119234.
- 146 [20] X. Chen, Y. Xu, M. Wen, Y. Wang, K. Pang, S. Wang, Q. Chu, D. Chen, *Combustion and*
147 *Flame* **2025**, *275*, 114065.
- 148 [21] Y. Xu, W. Sun, X. Chen, Y. Wang, W. Ji, D. Chen, *Chemical Engineering Science* **2025**, *310*,
149 121535.
- 150 [22] H. Stagge, R. Güttel, *Chemical Engineering Journal* **2025**, *510*, 161460.
- 151 [23] L. Luo, Q. Liu, J. Sun, Y. Huang, *Chemical Engineering Science* **2025**, *306*, 121307.
- 152 [24] J. Shukla, X. Qu, Z. Darbari, M. Iloska, J. A. Boscoboinik, Q. Wu, *Journal of Physical*
153 *Chemistry Letters* **2025**, *16*, 3562–3570.
- 154 [25] H. Chen, Q. Li, S. Deng, *Energy & Fuels* **2024**, *38*, 15630–15641.
- 155 [26] T. Kircher, F. A. Döppel, M. Votsmeier, *Chemical Engineering Journal* **2024**, *485*, 149863.
- 156 [27] T. Kircher, F. A. Döppel, M. Votsmeier in *Computer Aided Chemical Engineering*, **2024**,
157 pp. 817–822.
- 158 [28] A. Fedorov, A. Perechodjuk, D. Linke, *Chemical Engineering Journal* **2023**, *477*, 146869.
- 159 [29] F. Biermann, R. Uglietti, F. A. Döppel, T. Kircher, M. Bracconi, M. Maestri, M. Votsmeier,
160 *Chemical Engineering Journal* **2025**, *519*, 163598.
- 161 [30] J. Dumesic, *Journal of Catalysis* **1999**, *185*, 496–505.
- 162 [31] R. T. Chen, Y. Rubanova, J. Bettencourt, D. K. Duvenaud, *Advances in neural information*
163 *processing systems* **2018**, *31*.
- 164 [32] D. P. Searson, M. J. Willis, A. Wright in *Statistical Modelling of Molecular Descriptors in*
165 *QSAR/QSPR*, Vol. 2, Wiley, **2012**, pp. 327–348.